CHARACTERISATION OF AIR-BORNE NOISE BY A DUMMY-SOURCE APPROACH

A Lindberg, Goran Pavic, Q. Leclere

CHARACTERISATION OF AIR-BORNE NOISE BY A DUMMY-SOURCE APPROACH

A. Lindberg[1*], G. Pavić[1], and Q. Leclère[1]

[1] Laboratoire Vibrations Acoustique de l'INSA de Lyon,
25 bis, avenue Jean Capelle, 69621 VILLEURBANNE Cedex, FRANCE
Email: anders.lindberg@insa-lyon.fr

ABSTRACT

A proper characterisation of noise of a vibrating source has to take into account both radiation from the source and diffraction by its body in order to enable prediction of sound pressure of the source when inserted into a given acoustical space. A particular technique, named the dummy source approach, has been developed with the aim of characterising real noise sources. Here the original source is replaced by a closed rigid cabinet of similar size and shape - the dummy - equipped with several small flush-mounted drivers. The noise of the original source is measured first in a number of control points and the source strengths of the drivers are then identified by inversion. Once a source is experimentally characterised by its dummy, further noise prediction steps can be carried out in a fairly straightforward manner since the source is represented by a simple shape and its excitation is of monopole type. The paper introduces the concept of the dummy source and discusses criteria of its acoustical layout. A characterisation procedure is then carried out via a virtual experiment aimed at validating the approach. The approach is finally validated by experimental results.

1 INTRODUCTION

Synthesis of air-borne noise radiated by steady-state vibration of an industrial source such as a diesel engine is quite some challenge in noise and vibration engineering. Recently sound synthesis methods have been in development, aimed at either sound auralisation [1] or virtual noise prototyping [2, 3]. In [3] sound radiation by an electric engine was modelled using sound pressure - force transfer functions. The forces were quantified by a mobility approach in which the original source was characterised by free velocities. Frenne and Johansson [4] compared simplified source models for time-domain quantification of partial sources on a diesel engine, the latter represented by a combination of several point sources distributed on its surface. Vogt et al. [5] identified sound sources on the surface of a diesel engine mock-up by an inverse boundary element approach. This

optimisation procedure allows for the construction of efficient synthesis models. The purpose of this paper is to discuss basic aspects of air-borne noise characterisation using a so called dummy. The dummy can then be applied as a black-box source model in a synthesis scheme.

At low frequencies, for which the source is small compared to the acoustic wavelength, the source can be characterised as a monopole, a dipole, a quadrupole, or a combination of such volumeless sources [6]. At high frequencies, for which the body is large compared to the wavelength, the source can be characterised by its power output [7]. In the mid-frequency range, a model of a source can be based on its normal velocity distribution [5]. This is applicable if the mechanical impedance of the housing is high; i.e., the housing vibration does not depend on the acoustic environment.

Bobrovnitskii and Pavić [8] proposed an alternative airborne characterisation technique based on blocked pressure and source impedance across an enclosing surface. These source quantities were defined in terms of analytical spherical functions, but the technique requires a spherical chamber to be carried out in practice. Pavić later proposed [9] a further refined source model based on patch averaged blocked pressure, and patch averaged source impedance. In this case the measurement of blocked pressure is not restricted to a chamber of any particular shape. The advantage of the developed approaches is that they are general and can be applied to any noise source. The disadvantage is that the measurement of blocked pressure is rather cumbersome in practice.

In this paper an approach in which the original source is replaced by a particular substitute source, the dummy source, is proposed. The dummy is a rigid closed cabinet of similar but simpler shape than the original source. The dummy accounts for both radiation and diffraction by the source. Sound radiation by the dummy is achieved by a number of M drivers spread across its surface. The response of each driver of surface D is governed by the source strength amplitude $\hat{Q}$ it produces, the acoustic features of the observation space Ω, and diffraction by the dummy's body. The dummy source implies that the integral formulation of sound radiation [10, p. 8] is approximated by

$$\hat{p}(\mathbf{f}) \approx \sum_{m=1}^{M} Z(\mathbf{f} \mid \mathbf{s}_m)\hat{Q}(\mathbf{s}_m), \qquad \hat{Q}(\mathbf{s}_m) = \int_{D_m} \hat{v}_\perp dD_m. \tag{1}$$

Here, the transfer impedance (Green's function) $Z(\mathbf{f} \mid \mathbf{s})$ satisfies the conditions at the boundaries of the observation space but with the original source replaced by the dummy. Thus the original source is characterised by its dummy and its excitation is provided by a lookup table of frequency source strengths $\hat{Q}_1, \ldots, \hat{Q}_M$. The latter are obtained by an inverse technique. The synthesis of sound, e.g. at the operator's ear in a machine compartment, may be carried out given an additional transfer impedance describing sound propagation from the dummy's driver array to the ear's position.

2 THE DUMMY SOURCE APPROACH

There are several steps in the proposed approach. The first step is the design of the dummy. On the closed rigid surface S of the dummy a driver array of M simple sources with centres at $\mathbf{s}_1, \ldots, \mathbf{s}_M$ are prescribed. The geometric centres will be referred to as source points. The second step is the sampling of sound radiated by the vibrating body. This is done using a microphone array of N control points, located at $\mathbf{f}_1, \ldots, \mathbf{f}_N$ around the source. The third step is to establish the dummy's transfer matrix. This matrix relates each simple source on the dummy's surface to each field point in the observation space. The fourth step is the inversion which may be ill-conditioned. Tikhonov regularisation is applied to improve conditioning but any other suitable regularisation technique can be employed. The check of the dummy source is finally done by predicting the sound pressure at E error points scattered around the original source.

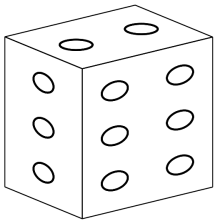

Figure 1. Schematic driver array set in a dummy's surface.

2.1 Design hypothesis

There is at beforehand no rational way to specify the number and positions of simple sources on the dummy. A hypothesis is that at least two sources per acoustic wavelength on the surface of the dummy are sufficient to reproduce far-field sound pressure of a vibrating body. This is different from other approaches such as e.g. boundary elements were often at least six elements per shortest acoustical or structural wavelength is required. The number of required sources M, and the average spacing δ between two adjacent source positions are roughly given by

$$M \approx 4S\frac{f_{\max}^2}{c^2}, \qquad \delta \approx \frac{c}{2f_{\max}} \tag{2}$$

where c is the speed of sound and S is the surface area of the dummy. Using the introduced criteria, a fixed grid of simple sources is prescribed. An acoustical layout, as used in this paper in section 4, with 22 drivers embedded in the surface of a closed rigid box - the dummy - is shown in Fig. 1. This satisfies the introduced criterion until 1000 Hz. The exact positions of the substitute sources are not so important as different layouts of identical number of sources will perform in a similar manner. Note the squared frequency dependence of the number of substitute sources needed by Eqs. 2 for the reproduction of sound. This hypothesis will be tested in two case studies.

2.2 Source identification

At a constant frequency, the pressure amplitudes at microphones in the observation space are put in a vector $\hat{\mathbf{p}}$ ($N \times 1$), and the unknown source strengths of the dummy's drivers are put in a vector $\hat{\mathbf{Q}}$ ($M \times 1$). The transfer impedance matrix $\mathbf{Z}$ ($N \times M$) is estimated using either repeated measurements or computations. Reciprocity may be used. The dummy's source strength distribution is quantified, at a constant frequency, by finding the solution to

$$\mathbf{Z}\hat{\mathbf{Q}} \approx \hat{\mathbf{p}}, \tag{3}$$

using a constrained least-squares approach [11, 12, 13]. To introduce the dummy source concept, it is here assumed that a smooth fit to the original sound field requires more control points than source points; i.e., $M \ll N$. The optimal number of microphones and their positions in the observation space represent a subject of its own which lies outside the scope of this paper.

Eq. 3 has no unique solution. This problem is overcome by being as close as possible in reproducing the original sound field while avoiding excessive source strengths of the simple sources. Such a trade-off can be expressed as

$$\hat{\mathbf{Q}} = \arg\min_{\beta} \|\mathbf{Z}\hat{\mathbf{Q}} - \hat{\mathbf{p}}\|_2^2 + \beta^2\|\hat{\mathbf{Q}}\|_2^2, \tag{4}$$

where β is the filtering parameter [12]. Hansen and O'Leary [11] proposed the L-curve to assess the filtering parameter. The best guess of filtering parameter corresponds to the value being closest to the corner of the L-curve, which can be identified by the largest curvature criterion [11]. Similar to the approach in [14], the curvature is found from central finite difference quotients. If the curve is concave, the Moore-Penrose pseudoinverse is used which finds the best fit solution to $\min \|\mathbf{Z}\hat{\mathbf{Q}} - \hat{\mathbf{p}}\|_2^2$.

2.3 Transfer impedances

An element of the transfer impedance (Green's function) matrix $\mathbf{Z}$ in Eq. 3, is given by

$$Z_{nm} = Z(\mathbf{f}_n \mid \mathbf{s}_m) = \frac{\hat{p}(\mathbf{f}_n)}{\hat{Q}(\mathbf{s}_m)}, \tag{5}$$

which respects the conditions at the boundaries of the observation space but with the original source replaced by the dummy. This function is not known. Two distinct approaches to the estimation of the dummy's transfer impedances are briefly described: (1) a numerical substitute source approach accounting for semi-anechoic condition of the surrounding space, and (2) an experimental approach using a source of known volume velocity. As a rule an experimental approach should be preferred since numerical modelling is difficult.

The two approaches are roughly equivalent inside of a semi-anechoic room. This has been deduced from repeated measurements with a dummy. Through the measurements it has been found that computed transfer impedances correspond in sound pressure level and phase to the experimental transfer impedances. Examples of experimental and numerical setups are shown in Fig. 2, and a sample transfer impedance is shown in Fig. 3. The deviations between computation and measurement are believed to be due to vibration of the dummy or imperfect room features. The characterisation method is described in [15].

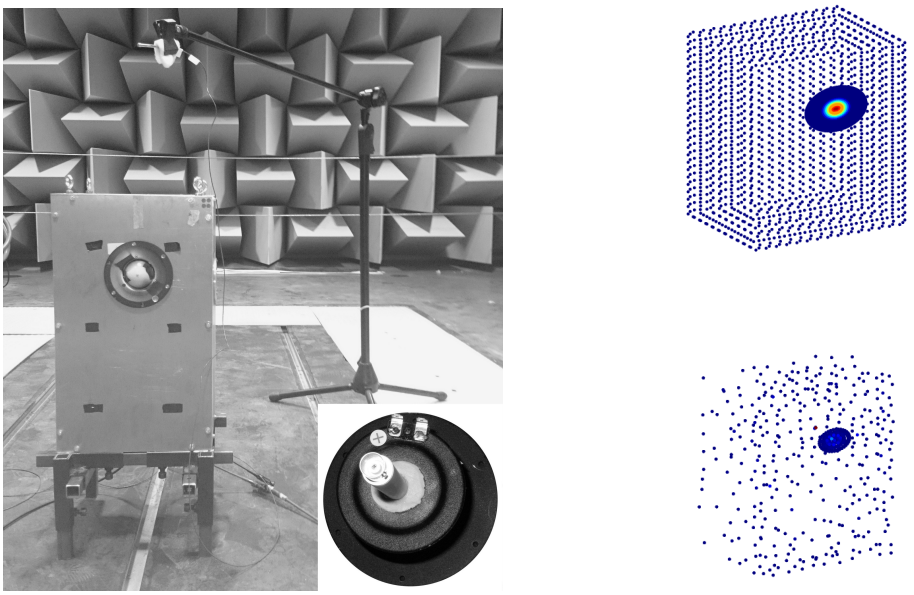

(a) (b)

Figure 2: Transfer impedance (a) measurement with a box using an instrumented driver shown in the lower right corner, and (b) computer model using a substitute source approach: upper part, points of prescribed velocity across the dummy's surface; lower part, positions of substitute monopole sources within the dummy at 525 Hz.

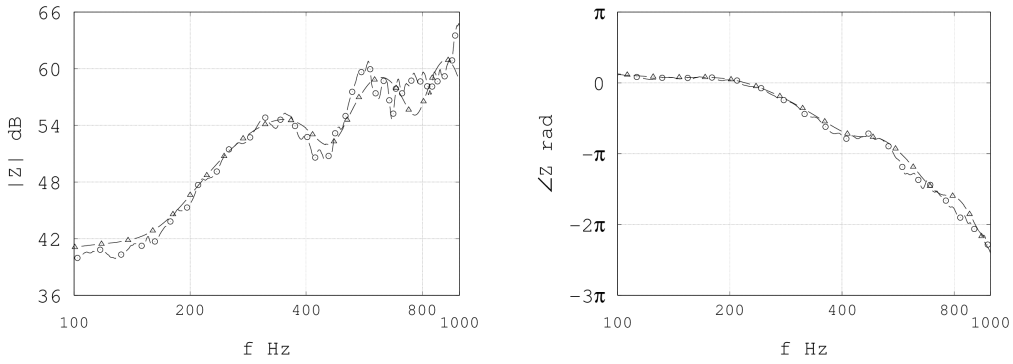

(a) (b)

Figure 3: Example transfer impedance (a) level dB re. 1 kg·m^{-4}·s^{-1} and (b) phase, legend: ∘ measured, △ computed.

2.3.1 Computation of transfer impedances

The dummy's cabinet surface C is assumed not to vibrate and acts only as an obstacle to the propagating sound. It follows that the normal component of particle velocity across the cabinet should vanish [6, pp. 100 - 103]. Let the driver be modelled by a circular disk of radius a in axisymmetric motion [16, 17]. A Greenspan [17] velocity profile $\zeta(\sigma)$ of the form

$$\zeta(\sigma) = \frac{1}{\pi a^2}(n+1)\left(1 - \frac{\sigma^2}{a^2}\right)^n, \tag{6}$$

which produce unit source strength is prescribed across the disk. Here, σ denotes the distance from a point $\mathbf{b}$ on the surface of the disk to the disk's geometric centre and n is the profile order. The normal velocity for the dummy's m^{th} simple source is

$$\mathbf{v}_\perp(\mathbf{s}_m) = \begin{cases} \zeta(\sigma_m),\ 0 \le \sigma_m \le a \\ 0, \text{otherwise on } S. \end{cases} \tag{7}$$

The radiated sound is computed using superposition of waves created by volumeless sources located inside of the dummy's surface [18, 19, 20, 21]. The particle velocity amplitude field created by the substitute sources has to reproduce the surface vibration amplitude field in the outward normal direction at any point on the closed surface of the dummy [18, 19]. The substitute source locations are chosen by a search algorithm [20] operating on a prescribed set of candidate source positions spread out within the entire dummy. This is the technique used in the computation of sound radiation. The computation is repeated for each source position on the dummy surface.

2.3.2 Measurement of transfer impedances

An experimental implementation of a simple source can be a small back-enclosed driver. A driver's diaphragm has low mechanical impedance and its volume velocity depends strongly on the acoustic environment. To overcome this problem the driver's source strength is deduced using a signal from an internal microphone [22, 23, 24]. The transfer impedance in Eq. 5 is split into two independent transfer functions: a source function and a space function. A driver's diaphragm is characterised by its source function. The volume velocity at the front of the driver's diaphragm, and thereby the source function, can be assessed in specific spaces where further substitution is possible. This can be achieved using a compression chamber or a blocked pipe [25, 26]. The advantage of these techniques are that no assumptions regarding the driver's diaphragm shape or velocity distribution are made. The identified source function is then applied in other spaces where the transfer impedance has to be measured.

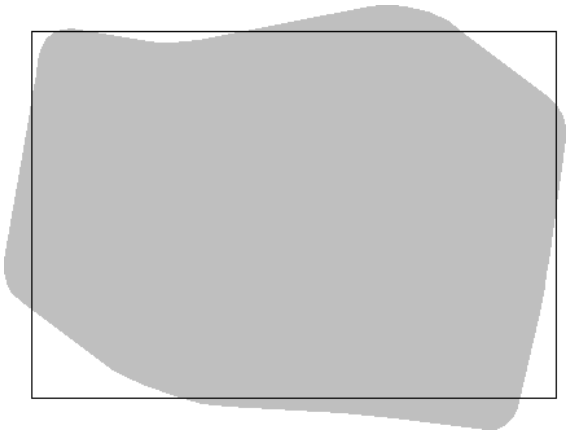

Figure 4: Schematics of the original source, grey area, and the dummy source's contour, black line, used for numerical evaluation.

3 NUMERICAL VALIDATION

The concept of a dummy source concerns any source radiating by vibration of its closed solid surface. The characterisation of air-borne noise aims at far-field radiation, and conserves only basic features: power output, directivity, and diffraction by the original source.

The matching between the sound field created by the original source and its dummy is here analysed in a two-dimensional case. The original source of irregular shape and its dummy of simple rectangular shape are shown in Fig. 4. This dummy will be equipped with a number of drivers positioned around its perimeter in an as equidistant way as possible. The size of the dummy, 500×350 mm, gives it an area equal to that of the original source; its centre coincides with the geometric centre of the original source.

The original source is constructed from a large number of line sources, the two-dimensional equivalent of monopoles, of randomly selected source strengths randomly scattered within the original source's contour [20]. The particle velocity of this field normal to the contour is identified. This velocity is thereafter taken as the normal vibration velocity of the original source since the field created by the internal line sources exactly matches the field created by the vibrating source outside its contour. The radiated field is then computed in a number of control points around the source. These points correspond to microphone positions in a real measurement setup.

Next the transfer impedances are computed between the pressure at control points and the unit source strengths at the drivers' positions. This computation is done using a technique described in [20]. The transfer impedance matrix obtained in this way is then used in an inverse computation to produce the source strengths of each driver. The field radiated by the dummy is finally obtained by superposing the individual fields of all the drivers. In the next sections basic results concerning sound scattering and sound radiation at a single frequency is given.

3.1 Sound scattering

Figures 5 compares the instantaneous values of pressure fields created by an external cylindrical source incident on the passive original source and the passive dummy at 500 Hz. The bodies are here acting only as obstacles to the propagating wave. A good matching between the two scattered fields is seen as expected. Close to the bodies the matching deteriorates somewhat due to the fine grained differences in the geometrical shapes, but the global features of the fields are the same. This illustrates that a field can be approximated by replacing the original body with its dummy. Diffraction of waves by the original source is therefore inherently taken into account by the dummy.

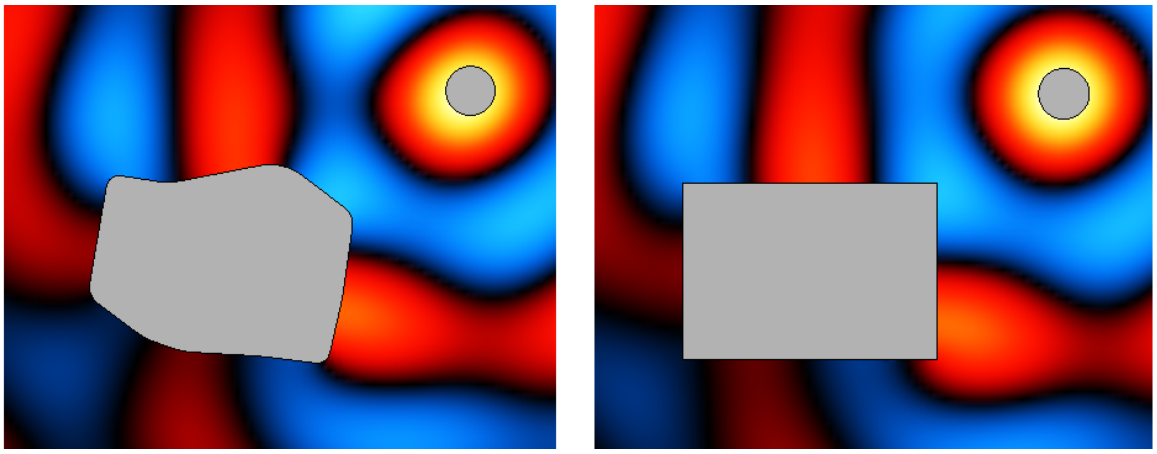

Figure 5: Scattering of sound by the original source, left, and by the dummy, right, at 500 Hz. Blue, negative; red, positive.

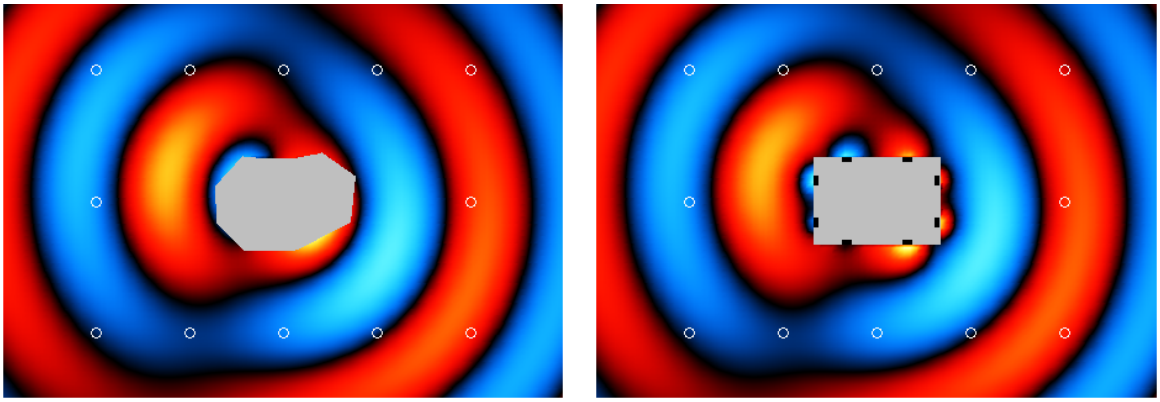

Figure 6: Radiation of sound by the original source, left, and by the dummy, right, at 500 Hz. White circles: control points; black spots: drivers.

3.2 Sound radiation

Figures 6 compares the instantaneous values of pressure fields created by the original source and the dummy at 500 Hz. The control points were distributed along a rectangular line 3 times larger than the contour line of the dummy source. The spacing between the control points was set to 62% of the wavelength, and the spacing between the drivers was set to 31% of the wavelength. These values were found to represent a reasonable trade-off between simplicity and accuracy, and were also applied at 250 and 1000 Hz.

The figures show a rather good matching of the two fields. Very close to the source the matching deteriorates due to high near-field gradients, but further away it improves a lot. The radiated powers of the original source and its dummy match extremely well, as shown in the Tab. 1.

Frequency (Hz)	Original source (W/m)	Dummy (W/m)
250	0.084	0.081
500	0.30	0.30
1000	0.91	0.92

Table 1. Power output by the two sources at some characteristic frequencies.

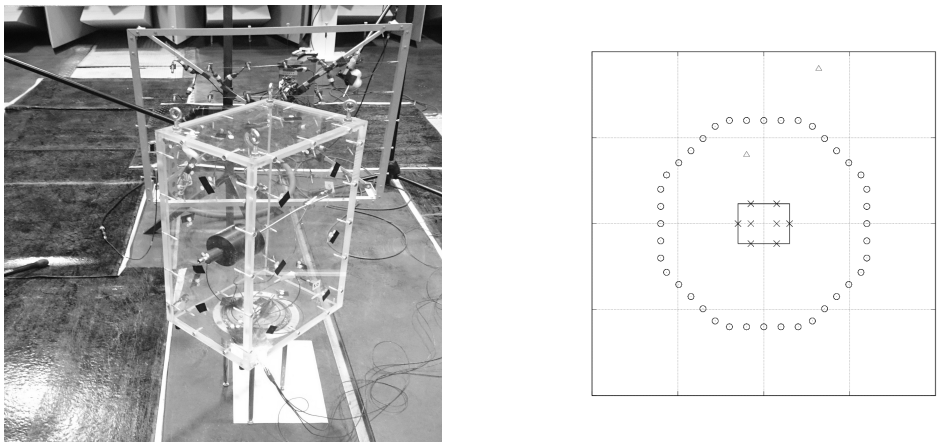

(a) (b)

Figure 7: Setup inside of a semi-anechoic room (a) array recording of the vibrating box using a turn table with the position of the substitute sources marked by black tape, and (b) schematic setup of control and error points (○), source points (×) and listening points (△) projected onto a plane.

4 EXPERIMENTAL VALIDATION

A box of dimensions $300 \times 232 \times 500$ mm was used as original source. The box was made out of six 12 mm thick Plexiglass plates, and excited using an electrodynamic shaker mounted inside of the box. This shaker was fed with low passed white noise. The vibrating box was mounted on a turn table at a height of 300 mm from the floor inside of a semi-anechoic room. The box was rotated such that 8 different 5×5 planar array recordings with an angular step of 45° were achieved. The array was positioned 600 mm from the box centre and the spacing between microphones was 100 mm. The height of the array was adjusted to coincide with the vibrating box. This resulted in 200 measurement points which were randomly split into 128 control points and 70 error points. Additional measurements were done at two listening points lying inside and outside of the virtual surface. The experimental setup is shown in Fig. 7.

A dummy of identical dimensions as the box was computer modelled. On the surface of the dummy a driver array with 22 sources was defined using Eq. 2. This fulfils the hypothesis of at least 2 sources per wavelength until 1000 Hz. The simple sources are spread across all faces of the dummy. The dummy was placed at a height of 300 mm from the ground in a virtual half-space, and thereafter the transfer impedances were computed using the approach outlined in section 2.3.1. The floor was modelled using the mirror image technique.

4.1 The box's response

The measured response was expressed as a pressure spectral density matrix $\mathbf{G}_{pp}$ $(N \times N)$ [27, pp. 391 - 409], which is related to the dummy's source strength spectral density matrix $\mathbf{G}_{QQ}$ $(M \times M)$ by the transfer impedance matrix $\mathbf{Z}$ as [13]:

$$\mathbf{G}_{pp} \approx \mathbf{Z}\mathbf{G}_{QQ}\mathbf{Z}^*, \tag{8}$$

the solution was obtained frequency by frequency using a least-squares approach. This equation is reformulated to the form of Eq. 3 by principal components [28]. The advantage of this approach is that the same numerical treatment can be applied on both Eq. 8 and Eq. 3. The disadvantage is that repeated matrix inversions for each principal component of interest are necessary. The unknown source strength matrix is then reconstructed from the identified principal source strength vectors.

Using several repeated array measurements synchronisation is required. In the specific case of the vibrating box this has been achieved by a reference signal. The n^{th} measurement signal was

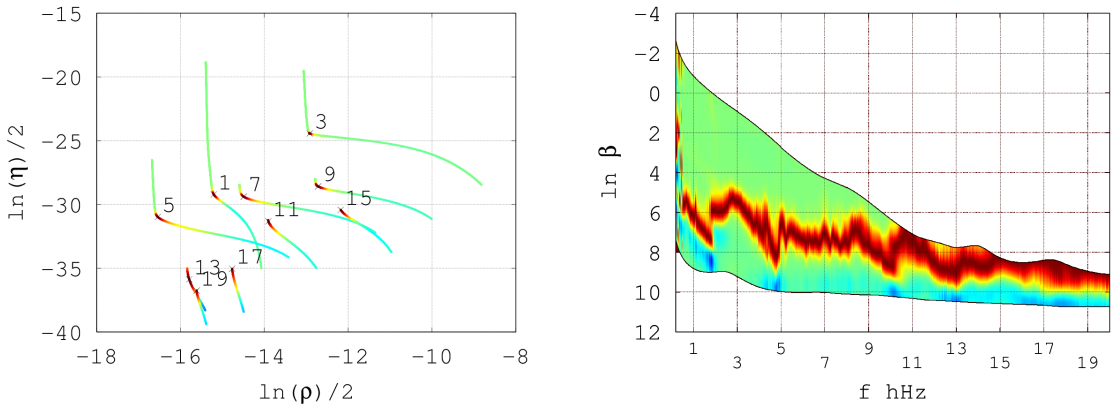

Figure 8: L-curves, left, with normalised curvature $\kappa/\max(|\kappa|)$ at 1, 3, ..., 19 hHz with the largest curvature indicated by an $\times$-marker, and a map, right, of normalised curvature as function of filtering parameter and frequency. Blue, negative; red, positive; green, zero.

synchronised using one reference signal r, the complex pressure amplitude is then given by

$$\hat{p}_n = \sqrt{2G_{nn}}\frac{G_{nr}}{|G_{nr}|}, \qquad \mathbf{G}_{pp} \approx \frac{1}{2}\hat{\mathbf{p}}\hat{\mathbf{p}}^*, \tag{9}$$

which can be used to approximate the full pressure spectral density matrix. The voltage signal feeding the shaker was used as a reference signal. Synchronisation was only carried out at control and error points. The pressure auto-spectral density at the listening points were computed separately from the time signals to check the results [27].

4.2 The dummy's source strengths

The dummy's source strengths were estimated from the measured pressure, Eq. 9, at the microphones using the outlined regularisation technique, Eq. 4, combined with computed transfer impedances of the dummy source, Eq. 7. Sample L-curves, the range of singular values and the curvature as function of frequency are shown in Fig. 8.

The selected filtering parameter is nearly continuous between 100 Hz and 2000 Hz. This indicates that the largest curvature criterion is applicable. It is seen that the transfer matrix is increasingly ill-conditioned with decreasing frequency, motivating the use of a regularisation technique. At higher frequencies there are small differences in the identified source strengths from that obtained by Moore-Penrose pseudoinversion.

4.3 Performance at error points

Once the vibrating box was characterised its dummy was used to predict the sound pressure at 70 independent error points. The error points are located at the same array as the control points, but they were not used in the inversion, and are used to check the dummy's performance. A first check is the dummy's far-field power output. This is related to the spatial averaged pressure at the error points. A comparison between the predicted and measured spatial averaged pressure, as well as pressure in one point, is shown in Fig. 9. Good matching between the box and the dummy is seen in the range 200 - 1000 Hz. Going below 200 Hz the box is not an efficient radiator of sound, while the room likely ceases to be semi-anechoic. This may explain the deviation in the dummy's behaviour at low frequencies apart from problems coming from inversion. The matching is however rather good down to about 80 Hz. Surprisingly, the matching in the range 1000 Hz to 2000 Hz is good suggesting that the hypothesis about the number of drivers, Eq. 2, may be

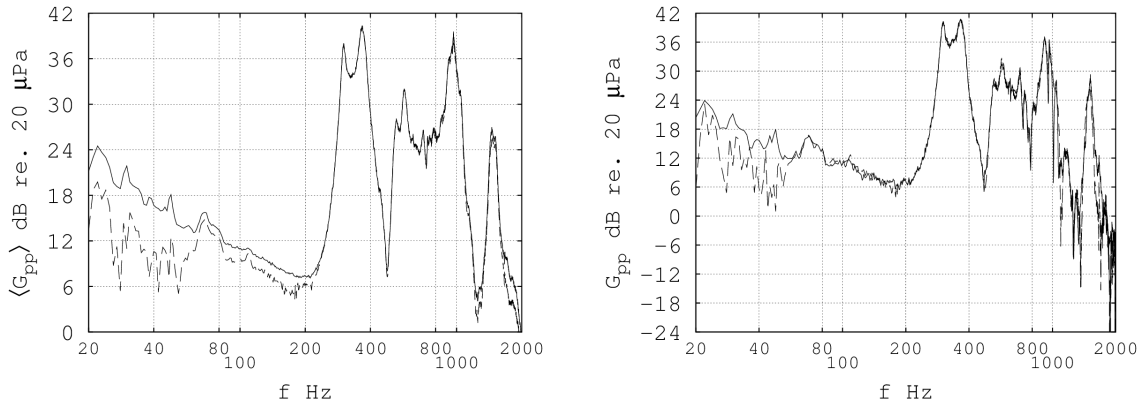

Figure 9: Performance at error points: left, spatial averaged pressure response; right, pressure response at one error point. Continuous line, vibrating box; dashed line, dummy source.

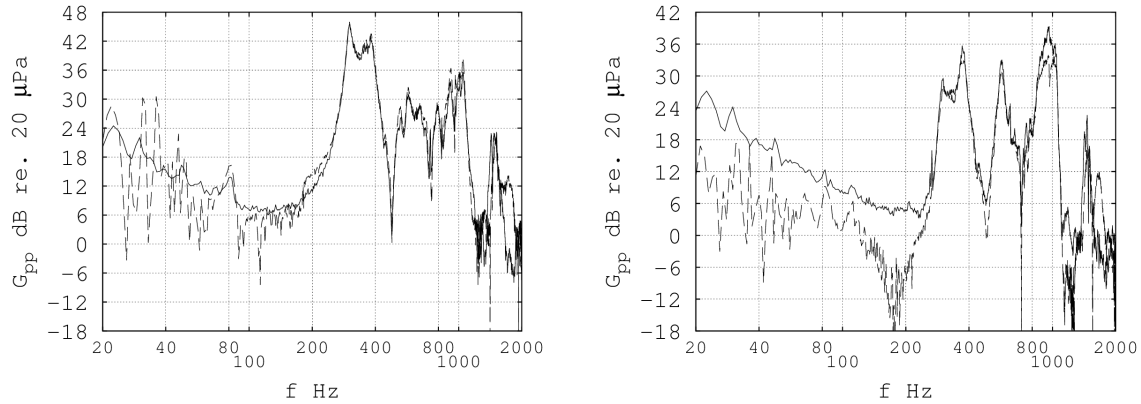

Figure 10: Performance at listening points: left, interior to virtual surface; right, exterior to virtual surface. Continuous line, vibrating box; dashed line, dummy source.

unnecessarily penalising in this particular case. The results indicates that the dummy can be used to predict both the power output and the pressure response.

4.4 Performance at listening points

To further investigate the performance of the dummy, predictions are made at listening points not located at the virtual surface of the array used to characterise the dummy. The result is shown in Fig. 10. Contrary to the case of error points, there are large level differences at some frequency ranges between the box and its dummy. It is seen that the radiated pressure by the dummy is reasonably close to the one radiated by the vibrating box between 200 Hz and 1000 Hz. This suggest that the hypothesis of 2 sources per smallest wavelength of interest is potentially applicable.

5 CONCLUDING REMARKS

A modelling concept believed to be applicable for prediction of noise radiated by a vibrating source of complex geometry has been proposed. The developed model is based on substitution of the real source with a closed rigid cabinet - the dummy - being of similar but simple shape. The dummy intrinsically models diffraction by the original source. Sound radiation by the original source is modelled by superposition of waves created by a number of drivers embedded in the dummy's surface. The dummy aims at preserving far-field radiation characteristics of the original source while simultaneously accounting for diffraction by the source.

The source strengths of the dummy's drivers are obtained by an inverse technique. At first response measurements are done using control microphones spread around the original source. Thereafter the dummy is introduced in the same environment at the place of the original source, and the dummy's transfer impedances relative to the control microphones are identified. Knowing the dummy's transfer impedances and the pressure response of the original source enables the inverse computation of the drivers' source strengths using a constrained least-squares approach.

To the best of the authors' knowledge, no simple optimisation procedure exists for finding the number of drivers and their positions needed for satisfactory sound reproduction. This problem has been overcome by use of a fixed array using two sources per acoustic wavelength. An optimised driver array would perform better, but it would also depend on the specific source and its operation. On the contrary, it is believed that a single dummy equipped with a fixed driver array may represent an entire class of real sources of similar size and shape in various operational conditions. This enables a comparison of different industrial sources mounted in a mechanical assembly.

Two different techniques for establishing the dummy's transfer impedances have been briefly described: (1) a numerical approach based on superposition of monopoles suitable for semi-anechoic conditions, and (2) an experimental approach applicable anywhere. The computational model of a driver in a cabinet above a rigid ground has been validated experimentally.

So far no conclusive findings about the number of drivers per acoustic wavelength has been made. In the experimental validation it seems like less than two sources per acoustic wavelength may be sufficient to match the power output. In simulations not presented in this paper, up to four sources per wavelengths have been required to accurately reproduce the sound field when the volume velocity of the original source is negligible. Thus, the design of the dummy's source array depends on the source in question and may require some trial and error engineering.

Finally, the approach has been validated experimentally in a semi-anechoic room using a medium-sized vibrating box as original source. The predicted and measured response shows satisfactory matching.

ACKNOWLEDGEMENTS

This work was co-funded by Volvo Construction Equipment. The funding and discussions with Nicklas Frenne and Catalin Badau are gratefully acknowledged. The work was carried out at Laboratoire Vibrations Acoustique at INSA de Lyon in France, a member of the Centre Lyonnais d'Acoustique. The experimental work has been greatly assisted by Patrick Blachier. Antonio Pereira has helped with comments about inversion.

REFERENCES

[1] D. Berckmans, B. Pluymers, P. Sas, and W. Desmet. Numerical comparison of different equivalent source models and source quantification techniques for use in sound synthesis systems. *Acta Acustica United Ac.*, 97:138–147, 2011.

[2] A. T. Moorhouse and G. Seiffert. Characterisation of an airborne sound source for use in a virtual acoustical prototype. *J. Sound Vib.*, 296:334–352, 2006.

[3] A. T. Moorhouse. Simplified calculation of structure-borne sound from an active machine component on a supporting substructure. *J. Sound Vib.*, 302:67–87, 2007.

[4] N. Frenne and Ö. Johansson. Acoustic time histories from vibrating surfaces of a diesel engine. *Appl. Acoust.*, 67:230 – 248, 2006.

[5] T. S. Vogt, C. Y. Glandier, J. Morkholt, A. Omrani, and M. A. Hamdi. Engine source identification using an i-bem technique. In *Proc. of the Euronoise*, pages 1–6, 2003.

[6] A. D. Pierce. *Acoustics - An Introduction to Its Physical Principles and Applications*. McGraw-Hill Book Company, 1981.

[7] I. L Vér and L. L. Beranek. *Noise and Vibration Control Engineering, 2^{nd} ed.* John Wiley & Sons, 2006.

[8] Y. Bobrovnitskii and G. Pavić. Modelling and characterization of airborne noise sources. *J. Sound Vib.*, 261:527–555, 2003.

[9] G. Pavić. Air-borne sound source characterization by patch impedance coupling approach. *J. Sound Vib.*, 329:4907–4921, 2010.

[10] M. C. Junger and D. Feit. *Sound, structures and their interaction*. The MIT Press, 1972.

[11] P. C. Hansen and D. P. O'Leary. The use of the l-curve in the regularization of discrete ill-posed problems. *J. Sci. Comput.*, 14:1487–1503, 1993.

[12] P. C. Hansen. The l-curve and its use in the numerical treatment of inverse problems. In *Computational Inverse Problems in Electrocardiology, ed. P. Johnston, Advances in Computational Bioengineering*, pages 119–142. WIT Press, 2000.

[13] P.A. Nelson and S. H. Yoon. Estimation of acoustic source strength by inverse methods: Part i, conditioning of the inverse problem. *Journal of Sound and Vibration*, 233:639 – 664, 2000.

[14] J.-L. Le Carrou, Q. Leclère, and F. Gautier. Some characteristics of the concert harp's acoustic radiation. *J. Acoust. Soc. Am.*, 127:3203–3211, 2010.

[15] A. Lindberg and G. Pavić. Experimental characterisation of a small compression driver. In *Proc. of the Congrés Français d'Acoustique (CFA)*, pages 1601–1607, 2014.

[16] D. L. Dekker, R. L. Piziali, and E. Dong. Effect of boundary conditions on the ultrasonic beam characteristics of circular disks. *J. Acoust. Soc. Am.*, 56:87–93, 1974.

[17] M. Greenspan. Piston radiator: Some extensions of the theory. *J. Acoust. Soc. Am.*, 65:608–621, 1979.

[18] L. Song, G. H. Koopmann, and J. B. Fahnline. A method for computing acoustic fields based on the principle of wave superposition. *J. Acoust. Soc. Am.*, 86:2433–2438, 1989.

[19] M. Ochmann. The source simulation technique for acoustic radiation problems. *Acustica*, 81:512–527, 1995.

[20] G. Pavić. An engineering technique for the computation of sound radiation by vibrating bodies using substitute sources. *Acta Acustica United Ac.*, 91:1–16, 2005.

[21] G. Pavić. A technique for the computation of sound radiation by vibrating bodies using multipole substitute sources. *Acta Acustica United Ac.*, 92:112–126, 2006.

[22] T. Salava. Sources of the constant volume velocity and their use for acoustic measurements. *J. Audio Eng. Soc.*, 22:146–153, 1974.

[23] T. Salava. Acoustic load and transfer functions in rooms at low frequencies. *J. Audio Eng. Soc.*, 36:763–775, 1988.

[24] D. K. Anthony and S. J. Elliott. A comparison of three methods of measuring the volume velocity of an acoustic source. *J. Audio Eng. Soc.*, 39:355–366, 1991.

[25] A. Lindberg and G. Pavić. Experimental characterisation of a small compression driver using an internal microphone. In *Proc. of the International Conference on Noise and Vibration Engineering (ISMA)*, pages 1111–1119, 2014.

[26] A. Lindberg and G. Pavić. Measurement of volume velocity of a small sound source. *Appl. Acoust.*, 91:25–32, 2015.

[27] J. S. Bendat and A. G. Piersol. *Random Data - Analysis and Measurement Procedures*. John Wiley & Sons, 1986.

[28] Q. Leclère, G. Pavić, and S. Greffe. Quantification of airborne and structureborne engine noise in a coach under real operating conditions. *Proc. of the International Conference on Noise and Vibration Engineering (ISMA)*, pages 3203–3211, 2008.